CONF-760424--11

LA-UR -76-830

TITLE: HYDRODYNAMICAL ASPECTS OF HEAVY-ION COLLISIONS

AUTHOR(S): A. J. Sierk and J. R. Nix

MASTER

Talk presented at

Symposium on Macroscopic Features of Heavy-Ion Collisions
Argonne National Laboratory
Argonne, Illinois 60439
April 1 - 3, 1976

los alamos
scientific laboratory
of the University of California
LOS ALAMOS, NEW MEXICO 87544

An Affirmative Action/Equal Opportunity Employer

UNITED STATES
ENERGY RESEARCH AND
DEVELOPMENT ADMINISTRATION
CONTRACT W-7405 ENG. 36

HYDRODYNAMICAL ASPECTS OF HEAVY-ION COLLISIONS*

A. J. Sierk† and J. R. Nix
W. K. Kellogg Radiation Laboratory
California Institute of Technology, Pasadena, California 91125
and
Theoretical Division, Los Alamos Scientific Laboratory
University of California, Los Alamos, New Mexico 87545

ABSTRACT

In the framework of a hydrodynamical model, we investigate three important aspects of heavy-ion collisions: the potential energy of a nucleus as a function of deformation, the dynamical coupling between collective shape modes, and the effect of the transfer of collective energy into single-particle excitations.

The dependence of potential energy on shape has the effect of preventing fusion of heavy ions unless the nuclear system can be brought inside its fission saddle point. For increasing mass number A and angular momentum the fission saddle-point shape becomes more compact than a touching-ion configuration, leading to a rapid drop of predicted fusion cross sections in the vicinity of A = 200.

For nuclei with $A \gtrsim 200$, the coupling between collective shape modes increases the kinetic energy needed by colliding ions to coalesce to a compact shape. This increases the energy required for fusion.

In addition to exciting collective shape oscillations during heavy-ion collisions, some of the initial kinetic energy is converted into internal single-particle excitation energy. We discuss two possible mechanisms for this conversion: ordinary (two-body) viscosity, which arises from collisions between individual nucleons, and one-body dissipation, which arises from nucleon collisions with the moving potential wall. Dynamical calculations using either of these dissipation mechanisms reproduce experimental fission-fragment kinetic energies for nuclei throughout the periodic table. Many of the experimentally observed features of strongly damped heavy-ion collisions are reproduced by dynamical calculations using relatively small values of the ordinary two-body viscosity coefficient, although some discrepancies remain. The analogous calculations using one-body dissipation are not yet done.

---

*This work was supported in part by the National Science Foundation [PHY76-02724] and by the U.S. Energy Research and Development Administration.
†Alfred P. Sloan Research Fellow.

1. INTRODUCTION

In studying large-scale nuclear collective motion such as occurs in fission and heavy-ion collisions, one is in general both unable and unwilling to follow in detail the time evolution of the many-body wave function. However, one usually measures only a few gross features of the reaction products, such as their masses and charges, kinetic energies, and angles. These quantities should depend primarily on a few important collective variables that describe the shape of the nucleus. Thus one is led to try to model such processes by solving dynamical equations for a small number of collective degrees of freedom, and to lump one's ignorance of the finer details of what is happening into such concepts as the dissipation of collective energy into excitation energy.

The simplest type of model which retains many of the features of interest is a hydrodynamical model, which assumes that the ignored information can be described by such classical concepts as viscosity, nuclear equation of state, etc. In this paper we discuss a hydrodynamical model of nuclear collective motion that approximates nuclear matter as an incompressible, nearly irrotational fluid.[1-3] We discuss the three aspects of the equations of motion — potential energy, kinetic energy, and dissipation — in Secs. 2, 3, and 4, respectively. In Sec. 5 some calculated results for fission and heavy-ion collisions are presented and compared to experimental data. Throughout the paper our primary emphasis is on those qualitative aspects of the results that do not depend on our specific model.

2. POTENTIAL ENERGY

In calculating the potential energy of nuclei as a function of shape, we include three macroscopic contributions: nuclear macroscopic energy, Coulomb energy, and rigid-body rotational energy. We neglect single-particle modifications to the potential energy for several reasons. First, for the moderate collective energies that we are considering ($\approx$ 0.1 to 5 MeV per nucleon), the resulting excitation energy of the nucleus should decrease the effect of the single-particle structure. Second, the qualitative effect of these modifications is to introduce a "ripple" with an amplitude of a few MeV into the potential-energy surface. When superimposed onto the large-scale potential-energy variations caused by the Coulomb and nuclear energies, these corrections have little influence on the large-scale dynamics except for important

effects near the ground state and fission saddle point. Finally, there is the important pragmatic consideration that the calculation of single-particle effects by one of the Strutinsky method[4,5] is too time consuming to be included in a dynamical calculation of fission or fusion.

For calculating the nuclear macroscopic energy of the nucleus, we replace the usual liquid-drop-model surface energy by a modification that includes effects of the finite range of the nuclear force.[6,7] This formulation results in a contribution to the energy whose leading shape-dependent term is proportional to the surface area of the nucleus. The additional correction terms vanish as the range of the force approaches zero, which means that in this limit the usual liquid-drop-model surface energy is recovered. The inclusion of these finite-range corrections leads to a more accurate reproduction of the energy of highly deformed shapes such as are encountered in the fusion of two nuclei or during the later stages of fission. The use of the finite-range energy in dynamical calculations leads to some significant differences[8] compared to the liquid-drop model.

We calculate the Coulomb energy for a uniform-charge-density, sharp-surfaced drop. Because the second-order surface-diffuseness correction to the Coulomb energy is independent of shape[9] and the third-order correction is proportional to the surface area,[10] this method takes into account implicitly the effect of the surface diffuseness on the Coulomb energy to third order in diffuseness.

For systems with angular momentum, we model its effects approximately by adding to the Coulomb and macroscopic nuclear potential energies a centrifugal pseudopotential calculated for a nucleus that is rotating as a rigid body. This approximation includes the important repulsive effect of angular momentum but neglects totally the effects of coriolis accelerations. The approximation is good for nearly head-on collisions but is questionable for large impact parameters.

If one defines a one-dimensional family of shapes, it is possible by use of these three contributions to the energy to calculate the familiar interaction barriers as functions of angular momentum for various systems.[7] However, for discussing the processes of fission and fusion it is important to consider a multidimensional potential-energy surface. In order to more easily present this information, we project the results of such multidimensional calculations onto a two-dimensional space of central moments.[2,3,7,11] For a

mass-symmetric shape we denote by $\langle z^n \rangle$ the average of z^n over the right half of the nucleus, where z is the distance from the plane bisecting the shape. The center-of-mass separation coordinate r is then defined by $r = 2\langle z \rangle$ and the fragment-elongation coordinate σ is defined by $\sigma = 2[\langle (z - \langle z \rangle)^2 \rangle]^{\frac{1}{2}}$. For equal spheroidal fragments, r is the distance between their centers of mass, and σ is proportional to the semisymmetry axis of each spheroid.

In Fig. 1 we present a contour plot in r-σ space of the macroscopic potential energy for a ^{220}U nucleus with zero angular momentum.[11] Some of the more important items on this figure are the two-fragment valley, the shallow region near the spherical ground state where the neglected single-particle effects would be most important, the fission saddle point at the outlet of this "ground-state lake," the slight ridge separating the upper fusion valley from the fission valley, and the location of the tangent-sphere configuration.

For zero angular momentum, the fission saddle point occurs where the slope of the nuclear energy as a function of increasing deformation is equal to the negative of the slope of the decreasing Coulomb energy. As one considers heavier systems, where the Coulomb energy increasingly dominates, the saddle-point configurations therefore grow more compact. This is illustrated in Fig. 2, where we plot in r-σ space the locations of the macroscopic-energy saddle points for various systems. Note how the saddle-point shape is nearly spherical for heavy nuclei, while it is quite elongated for light nuclei.

Of particular importance is the location of the fission saddle point relative to the contact point of two ions forming the total system. Note that when two <u>light</u> ions are brought into contact they are already <u>inside</u> the fission saddle point, and will thus form a compound system. This is true for all systems with less than about 200 nucleons at moderately small bombarding energies. In order to achieve fusion, one has only to bring the ions over the fusion-valley interaction barrier, which means that a reasonable one-dimensional model of the potential energy as a function of ion separation will result in a correct prediction of fusion cross sections for relatively low energies. In this case, consideration of the dynamical evolution of the system after contact is unnecessary.

The effect of angular momentum is qualitatively similar to the effect of the Coulomb energy. Because the centrifugal potential is repulsive, this means that increasing the angular momentum of a given nucleus will cause its fission saddle point to become more compact. There exists a limiting angular

momentum at which the saddle point disappears (the ground-state shape is the same as the saddle-point shape for this value of angular momentum).[12] For angular momenta above this critical value, a compound nucleus cannot be formed, so higher-energy fusion cross sections for intermediate-weight nuclei are limited by this angular-momentum cutoff.

For systems with more than about 200 nucleons, the situation changes significantly, with the result that one-dimensional barrier calculations are irrelevant to fusion. Extrapolation to heavy systems of results from light ones will be incorrect, because different mechanisms dominate in the different mass regions. The question of whether or not a particular partial wave will fuse must be answered by considering the dynamics of the motion after the ions come into contact.

3. KINETIC ENERGY

It is well known that the dynamical evolution of a system is not determined only by the potential-energy surface. The equations of motion for a non-dissipative system may be written in a form exhibiting the fact that the dynamical trajectories are the geodesics of the non-Euclidean space of collective coordinates for which the inertia tensor is the metric.

In our hydrodynamical model, we calculate the inertia tensor by specifying the internal matter flow for a given shape variation. We describe the nuclear shape by the coordinates $q = q_1, \ldots, q_n$ corresponding to the three-quadratic-surface shape parameterization.[1,3] The kinetic energy is then equal to

$$T(q,\dot{q}) = \frac{1}{2} \Sigma M_{ij}(q)\, \dot{q}_i\, \dot{q}_j = \frac{1}{2} \rho \int v^2\, d^3x \quad .$$

Here M_{ij} is an element of the inertia tensor, $\dot{q}_i$ is the time derivative of the coordinate q_i, ρ is the mass density of the matter, $\vec{v}$ is the internal velocity of the fluid, and the integral is over the entire volume of the drop. We assume that $\vec{v}$ is irrotational and approximate the irrotational flow by means of the Werner-Wheeler method.[1,3] Although it is known that the inertia for small-scale motion near the ground state of a cool nucleus is several times as large as the irrotational value, the inertia for highly excited nuclei and for large deformation should be closer to the irrotational value.[5,7] In addition, for classical systems the irrotational inertia is a strict lower limit to the correct value.[13] The results calculated in a

hydrodynamical model obviously depend on the choice of internal flow, but many of the qualitative features should nevertheless be valid for real systems.

Because the inertia tensor is non-diagonal and varies with position, energy is coupled between collective modes. For example, when two ions collide, they have all their energy initially concentrated in the relative motion of their centers of mass. As the ions coalesce, the energy is coupled into various shape oscillations, which reduces the amount of energy in the relative center-of-mass motion. When added to the repulsive effects of the Coulomb and centrifugal energies, this loss of energy in the fusion mode can prevent fusion from occurring, even when there is no dissipation present. This effect is due entirely to the nature of the inertia tensor.

In Fig. 3 we plot in r-σ space some calculated dynamical trajectories for nonviscous ^{110}Pd + ^{110}Pd collisions. The bombarding energy corresponds to 20 MeV of kinetic energy in the center-of-mass system relative to the top of the $l = 0$ interaction barrier. We see that the trajectories for low angular momentum pass inside the corresponding saddle points, but that above $l = 45$ the trajectories pass outside the saddle points, with the system quickly reseparating without forming a compound nucleus. There are two important effects operating: (1) the movement inward of the saddle point as the angular momentum increases, and (2) the movement outward of the dynamical trajectories. This latter effect arises primarily because the rotational energy decreases the kinetic energy available in the rotating frame of the nucleus.

We assume that partial waves either lead to compound-nucleus formation or not depending upon whether their trajectories pass inside or outside the fission saddle point. The resulting cross section for compound-nucleus formation is shown as a function of energy in Fig. 4. We also show for comparison the results of a one-dimensional model, where the critical angular momentum for a given energy is that which just allows the system to get over the one-dimensional interaction barrier or for which the effective potential after contact corresponding to that angular momentum is just attractive.[7] We see that the neglect of deformation effects gives rise to a predicted fusion cross section about 4 times as large as that calculated in a model with more than one dimension. Finally, the total reaction cross section is roughly 10 times the compound-nucleus cross section.

In Fig. 5 we plot the calculated compound-nucleus cross sections as a function of energy in excess of the $l = 0$ interaction barrier for the systems ^{200}Po, ^{220}U, and ^{248}Fm, which are formed in the symmetric collisions of ^{100}Mo, ^{110}Pd, and ^{124}Sn, respectively. We observe that during the relatively small change from A = 200 to 248, the compound-nucleus cross section drops rapidly, and the threshold energy moves significantly above the barrier energy.

We emphasize that the effects considered in this section inhibit fusion for heavy systems only, but that they apply to systems with zero dissipation. In the next section we examine the modifications caused by the dissipation of energy of collective motion into internal excitation energy.

4. DISSIPATION

In principle, if we could solve the exact dynamical equations corresponding to all the nucleons in the nucleus, there would be no dissipation, since energy is conserved in isolated systems. In the language of Sec. 3, we would say that all modes are coupled, and we could then investigate the energy in each mode as a function of time. Because in our hydrodynamical model we consider explicitly only a few collective variables, we treat all coupling of energy to short-wavelength collective modes and to single-particle excitations as irreversible loss of energy from the few degrees of freedom being followed in detail.

The actual method of calculation is to compute and include the Rayleigh dissipation function in the modified Lagrange equations of the system. The Rayleigh dissipation function is defined by

$$F = -\frac{1}{2}\,\frac{dE_{\text{collective}}}{dt} = \frac{1}{2}\,\Sigma\,\eta_{ij}(q)\,\dot{q}_i\,\dot{q}_j \quad ,$$

where $dE_{\text{collective}}/dt$ is the time rate of change of total energy in the collective variables considered and η_{ij} is an element of the viscosity tensor. The generalized force in the ith direction due to viscosity is then $-\Sigma\,\eta_{ij}\,\dot{q}_j$.

Qualitatively, the effect of dissipation is to slow down the dynamical motion, change the trajectories from non-dissipative paths in such a manner as to reduce the amount of dissipation, and to heat up the nucleus. This should reduce the single-particle effects on the potential energy and inertia, improving the validity of the macroscopic approach, wherein we have neglected all single-particle structure. The effect on the trajectories may also be thought of as the influence of the non-diagonal viscosity tensor, which is

analogous to the effect of the inertia tensor discussed in Sec. 3.

We now address the question of the nature of the dissipation mechanism. In a classical fluid, the dissipation is due to ordinary shear viscosity, which acts against gradients in the velocity. On a molecular level, this type of dissipation arises from binary collisions between individual molecules, which results in a diffusion of momentum between regions of differing velocity. We refer to this mechanism as two-body viscosity since it arises from two-body collisions between the molecules making up the fluid.

Since nucleons are thought to have long mean-free paths in nuclei, this mechanism of two-body viscosity might not be dominant. An alternative excitation mechanism which can occur in a collisionless classical gas is the transfer of energy to the gas by molecular collisions with a moving wall surrounding the gas. This process we refer to as one-body dissipation, since the energy loss is due to single particles colliding with the moving wall.[14-18]

Deciding whether either of these mechanisms is appropriate for nuclei might be possible after comparing calculated results to experimental results. We discuss in the next section some of the results of our dynamical calculations for nuclei with dissipation present.

5. CALCULATED RESULTS FOR DISSIPATIVE SYSTEMS

Using the method outlined in the preceeding three sections, we calculate first the most probable dynamical paths from the macroscopic fission saddle point to infinite fragment separation[3] for different values of the two-body viscosity coefficient μ. In Fig. 6 the [illegible] kinetic energies calculated in this model are plotted for several v[illegible] μ as functions of $Z^2/A^{1/3}$ for nuclei along Green's approximation to the [illegible] of beta stability.[19] The experimental data for symmetric fission of excited nuclei are also plotted in this figure. With a single value of viscosity (μ = 0.015 ± .005 TP = $9 \pm 3 \times 10^{-24}$ MeV s/fm^3), we obtain a good fit to the data, although there appears to be a systematic variation toward higher viscosity for heavier systems. This may be due to the neglect of angular momentum in the calculated results, which would have a greater effect for the lighter systems. The value of 1.5×10^{10} poise for the two-body viscosity coefficient provides less insight into the effect of viscosity on nuclear dynamics than does the observation that this value of viscosity is about 30% of the amount required to critically damp the quadrupole oscillations of an idealized heavy actinide nucleus.

Thus, experimental fission-fragment kinetic-energy data are reproduced by a moderately low value of two-body viscosity.

We switch our discussion now to the second type of dissipation mechanism. For a system initially at rest in thermal equlibrium, the one-body dissipation rate is proportional to the integral over the nuclear surface of the square of the normal velocity of the surface.[17,18] Because of the simplicity of the viscosity tensor, it is relatively easy to incorporate this model into dynamical calculations.[18] However, this approximation becomes unsatisfactory for the large deformations encountered during the later stages of fission, and is incorrect from the beginning of a heavy-ion collision. Among other inaccuracies, this model gives dissipation for simple center-of-mass translation. It is possible to modify this model to eliminate some of its faults,[20] but we have not yet calculated the results of such a modification. Instead, we present here the results corresponding to the original one-body dissipation formula.[17,18] This one-body dissipation formula contains no adjustable parameters, and for a Fermi-gas model of the nucleus the resulting rate of dissipation corresponds to a very overdamped system. As shown in Fig. 7, this model of a highly dissipative system also reproduces the experimental fission-fragment kinetic-energy data.[18]

The two types of dissipation exhibit very different effects in arriving at approximately the same result for the fragment kinetic energies. Two-body viscosity inhibits neck formation more than elongation, which makes the scission configuration more elongated than is the case for no dissipation.[3] This configuration has less Coulomb interaction energy and also somewhat less prescission translational kinetic energy than does the nonviscous ones. For the value μ = 0.015 TP, the final kinetic energy at infinity is approximately equal to the experimental results. One-body dissipation, on the other hand, inhibits elongation more than neck formation, which leads to a very compact scission shape. The dissipation is so high that there is almost no translational kinetic energy at scission. However, because the shape is so compact, the Coulomb interaction energy is much higher than in the nonviscous case. Without the use of any adjustable parameters, the calculated total energies at infinite fragment separation are almost equal to the experimental ones. The qualitatively different scission shapes corresponding to the two types of dissipation illustrate the strong effect on the dynamics of the form of the viscosity tensor.

As an example of a more complicated heavy-ion-collision process, we now

present a calculation of strongly damped collisions of ^{84}Kr with ^{209}Bi. In Fig. 3 we show the shapes of the system as a function of time for 600 MeV (lab.) ^{84}Kr bombarding ^{209}Bi with an angular momentum of 200 ħ, which is near the grazing angular momentum. The two-body viscosity coefficient has the value μ = 0.015 TP, and the system is started at rest in the rotating reference frame with a 2.0 fm neck radius at time T = 0. The use of this starting condition corresponds to the colliding nuclei being brought quickly to rest while maintaining spherical shapes during the early stages of neck formation, where the flow is not expected to be irrotational and incompressible.

The results of two similar calculations for ℓ = 0 and ℓ = 200 ħ are shown in Table I, where we also present for comparison some experimental data from the same reaction.[21] Although deficient in some respects, the calculated results nevertheless show many of the observed features. To begin with, the final fragment energy is reproduced quite well with the moderately low viscosity of μ = 0.015 TP. However, we must emphasize that we assumed that the radial motion was stopped before T = 0, and have not described a mechanism for this process. The lower-angular-momentum case leads to a lower energy, a larger mass transfer, and a larger scattering angle, which are all qualitatively in agreement with the experimental results for a larger scattering angle. However, the calculated mass transfer is too large, ranging from 24 to 42 amu, an amount to be compared to experimental results of 7 and 23 amu at center-of-mass scattering angles of 52° and 86°, respectively.

Table I. Some experimental and calculated results for strongly damped collisions of 600 MeV (lab.) ^{84}Kr on ^{209}Bi.‡

	Experimental Lab. angle = 34° Lab. angle = 59°	Calculated (μ = 0.015 TP) ℓ = 200 ħ ℓ = 0
C. M. scattering angle	52° 86°	53° 180°
Kinetic energy (MeV)	290 275	288 268
Mass transfer (amu)	7 23	24 42

[‡] The experimental kinetic-energy and mass-transfer entries are for the peak of the experimental distributions at the corresponding scattering angles.[21] The angular momentum value of 200 $\hbar$ was chosen for the first calculation since it is near the grazing angular momentum. The near equality of the scattering angles is fortuitous, since the experimental results could have been presented for other angles. The value of $l = 0$ was chosen for the second calculation to define the maximum range of mass transfer in the calculated collisions, not to try to duplicate the larger-angle experimental results.

Our results are very preliminary, but nevertheless allow us to make some comments. First, the experimental results for strongly damped collisions do not require that nuclei be very viscous (highly overdamped collective motion). Second, to reproduce experimental mass transfers for strongly damped collisions requires a form of dissipation that hinders mass transfer more than elongation.

6. SUMMARY AND CONCLUSION

We have discussed the three important contributions to the equations of motion for collective shape variations of nuclei: potential energy, kinetic energy, and dissipation (coupling to noncollective motion). An important effect of the potential-energy surface is to define the degree of compactness to which a nuclear system must be driven in order to form a compound nucleus. The coupling of various collective modes through the shape dependence and nondiagonality of the inertia tensor makes it necessary to supplement the information of the potential-energy surface by solving the dynamical equations of the nuclear system. The details of these dynamical couplings are important in the determination of the collision energy needed to cause complete fusion of heavy ions.

Dissipative effects cause further modifications of the dynamical trajectories; these modifications are quite different for different mechanisms of dissipation. We reproduce many of the experimentally observed features of fission and strongly damped heavy-ion collisions by calculations in a hydrodynamical treatment that models in a simplified way these three contributions to the dynamical equations of nuclear systems. However, some discrepancies remain.

By making further detailed comparisons with experimental results, we hope to establish limits to our hydrodynamical model and to possibly determine the best classical model and the necessary parameters for nuclear dissipation. We may also use the results of microscopic theories to modify the classical model.

This includes, for example, the use of the cranking model to calculate the inertia tensor, or, as we have already discussed, the incorporation of finite-range corrections to the liquid-drop-model surface energy. It may be possible to describe the overall collective behavior of a large class of reactions with a simplified model that allows us to do calculations with a reasonable amount of time and effort.

ACKNOWLEDGMENTS

We are grateful to Peter Möller for allowing us to use the contour plot of the ^{220}U potential energy. Our understanding of one-body dissipation has benefitted from discussion with W. J. Swiatecki and S. E. Koonin.

REFERENCES

1. J. R. Nix, Nucl. Phys. A130, 241 (1969); Lawrence Berkeley Laboratory Report No. UCRL-17958, 1968 (unpublished).
2. A. J. Sierk and J. R. Nix, in Proceedings of the Third International Atomic Energy Agency Symposium on the Physics and Chemistry of Fission, Rochester, New York, 1973 (International Atomic Energy Agency, Vienna, 1974), Vol. II, p. 273.
3. K. T. R. Davies, A. J. Sierk, and J. R. Nix, Phys. Rev. C (to be published).
4. M. Brack, J. Damgaard, A. S. Jensen, H. C. Pauli, V. M. Strutinsky, and C. Y. Wong, Rev. Mod. Phys. 44, 320 (1972).
5. J. R. Nix, Ann. Rev. Nucl. Sci. 22, 65 (1972).
6. H. J. Krappe and J. R. Nix, in Proceedings of the Third International Atomic Energy Agency Symposium on the Physics and Chemistry of Fission, Rochester, New York, 1973 (see Ref. 2), Vol. I, p. 159.
7. J. R. Nix and A. J. Sierk, Phys. Scr. 10A, 94 (1974).
8. A. J. Sierk and J. R. Nix, Kellogg Radiation Laboratory report (to appear).
9. W. D. Myers and W. J. Swiatecki, Nucl. Phys. 81, 1 (1966).
10. K. T. R. Davies and J. R. Nix, Los Alamos Scientific Laboratory report (to appear).
11. P. Möller and J. R. Nix, Los Alamos Scientific Laboratory Report No. LA-UR-76-416, 1976 (unpublished).
12. S. Cohen, F. Plasil, and W. J. Swiatecki, Ann. Phys. (N.Y.) 82, 557 (1974).
13. H. Lamb, Hydrodynamics (Dover, New York, 1945), 6th ed., Sec. 45, pp. 47-48.
14. G. Wegmann, Phys. Lett. 50B, 327 (1974).
15. G. Wegmann, in Proceedings of the International Workshop III on Gross Properties of Nuclei and Nuclear Excitations, Hirschegg, Kleinwalsertal, Austria, 1975, edited by W. D. Myers [Technische Hochschule Darmstadt Report No. AED-Conf-75-009-000, 1975 (unpublished)], p. 28.
16. D. H. E. Gross, Nucl. Phys. A240, 472 (1975).
17. W. J. Swiatecki, Lawrence Berkeley Laboratory Report No. LBL-4296, 1975 (unpublished).
18. J. Błocki et al., Lawrence Berkeley Laboratory report (to appear).
19. A. E. S. Green, Nuclear Physics (McGraw-Hill, New York, 1955), pp. 185, 250.
20. S. E. Koonin, 1976 (personal communication).
21. K. L. Wolf, J. P. Unik, J. R. Huizenga, J. Birkelund, H. Freiesleben, and V. E. Viola, Phys. Rev. Lett. 33, 1105 (1974).

FIGURE CAPTIONS

Fig. 1. Potential-energy contours for ^{220}U, in units of MeV.[11] The separation coordinate r is the distance between the centers of mass of the two halves of the system, and the fragment-elongation coordinate σ is the sum of the root-mean-square extensions along the symmetry axis of the mass of each half about its center of mass. These coordinates are measured in units of the radius R_0 of the spherical ^{220}U nucleus.

Fig. 2. Positions in r-σ space of fission saddle points for various nuclear systems with zero angular momentum. The isotopes chosen are those which could be formed in a symmetric binary collision of neutron-rich beta-stable nuclei. The saddle points for systems with less than about 200 nucleons are more elongated than the contact point, while those for heavier systems are more compact.

Fig. 3. Calculated dynamical trajectories for the reaction $^{110}Pd + {}^{110}Pd \rightarrow {}^{220}U$. The bombarding energy in the center-of-mass system is 20 MeV above the maximum in the one-dimensional zero-angular-momentum interaction barrier. The nuclear viscosity coefficient is zero, and single-particle effects are neglected. Only those trajectories with angular momentum ℓ less than the critical value $\ell_{crit} = 45$ pass inside the fission saddle point for that angular momentum (indicated by the points) and lead to compound-nucleus formation.

Fig. 4. Comparison of various cross sections for the reaction $^{110}Pd + {}^{110}Pd \rightarrow {}^{220}U$. The results are plotted as functions of the center-of-mass bombarding energy relative to the maximum in the one-dimensional zero-angular-momentum interaction barrier. In the energy region below the arrow in the solid curve the compound-nucleus cross section is determined by the requirement that the dynamical trajectory pass inside the fission saddle point, whereas at higher energies it is determined by the angular momentum at which the saddle point disappears. The dashed curve gives the compound-nucleus cross section calculated in terms of a one-dimensional interaction barrier, and the dot-dashed curve gives the total reaction cross section.

Fig. 5. Dependence of the compound-nucleus cross section upon the nuclear system. In the energy region below the first arrow in the top curve the cross section is determined by the one-dimensional interaction barrier. In the energy region between the two arrows in the top curve (and below the arrow in the two bottom curves) the cross section is determined by the requirement that the dynamical trajectory pass inside the fission saddle point. At higher energies the cross section is determined by the angular momentum at which the saddle point disappears.

Fig. 6. Comparison of experimental most probable fission-fragment kinetic energies with results calculated for different values of the two-body viscosity coefficient μ (solid curves). The calculations include the effect of the finite range of the nuclear force on the nuclear macroscopic energy. The experimental data are for the fission of nuclei at high excitation energies, where the most probable mass division is into two equal fragments. The open symbols represent values for equal mass divisions only and the solid symbols represent values averaged over all mass divisions. The dashed curves give the calculated translational kinetic energies acquired prior to scission.

Fig. 7. Comparison of experimental most probable fission-fragment kinetic energies with results calculated for one-body dissipation. The strength of the dissipation is determined from a Fermi-gas model of the nucleus. This dissipation corresponds to a very overdamped system. The results for infinite two-body viscosity are shown as a dashed line to illustrate the different effects of large dissipation in the two models. The experimental points are the same as in Fig. 6.

Fig. 8. Calculated shapes as a function of time for 600 MeV (lab.) ^{84}Kr bombarding ^{209}Bi with an angular momentu. of 200 ħ. The value of the two-body viscosity coefficient ' ₁ = 0.015 TP. At T = 0 the system was started from rest in the f of reference rotating with the system with a neck radius of 2.(₁. The Kr ion was initially incident from the left side of the f. ₁, along a path asymptotically parallel to the top of the figure. .. indicated in Table I, the final center-of-mass kinetic energy is 288 MeV, the final center-of-mass scattering angle is 53°, and the final masses of the fragments are 108 and 185 amu.

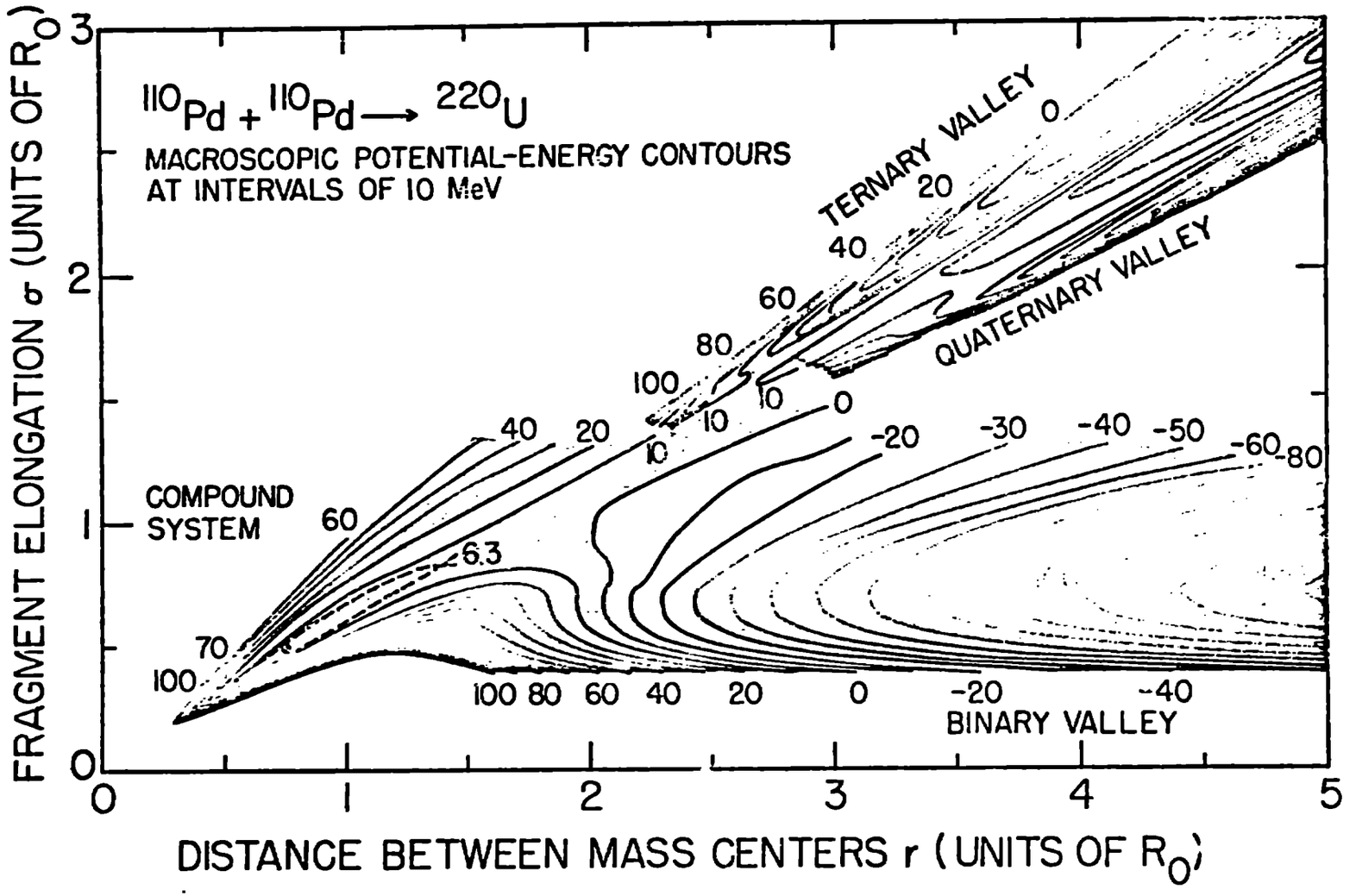
$^{110}Pd + ^{110}Pd \longrightarrow ^{220}U$
MACROSCOPIC POTENTIAL-ENERGY CONTOURS
AT INTERVALS OF 10 MeV
TERNARY VALLEY
QUATERNARY VALLEY
COMPOUND SYSTEM
BINARY VALLEY
FRAGMENT ELONGATION σ (UNITS OF R_0)
DISTANCE BETWEEN MASS CENTERS r (UNITS OF R_0)

FIG. 1

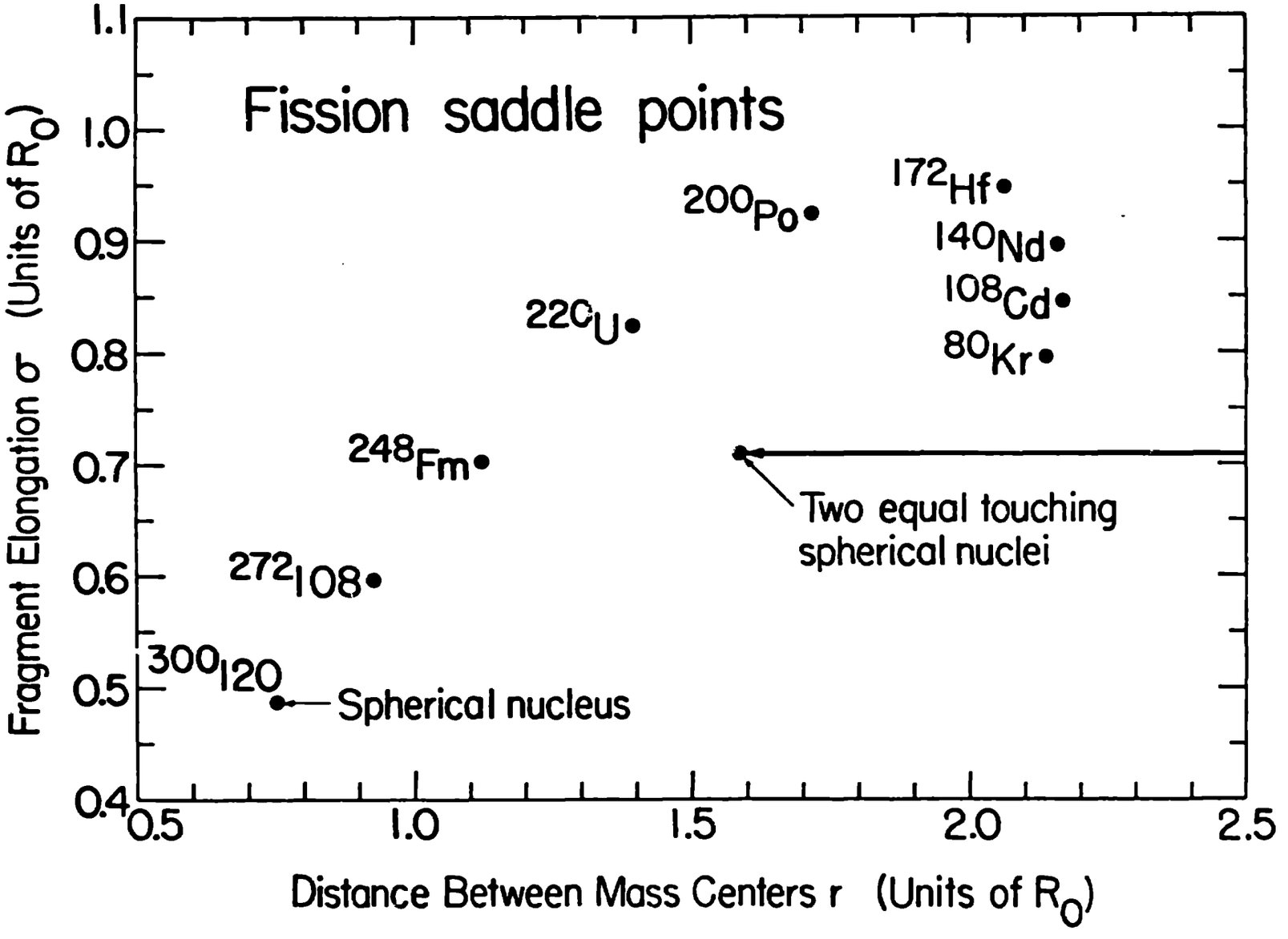
Fission saddle points
Fragment Elongation σ (Units of R_0)
Distance Between Mass Centers r (Units of R_0)
1.1
1.0
0.9
0.8
0.7
0.6
0.5
0.4
0.5
1.0
1.5
2.0
2.5
^{172}Hf
^{200}Po
^{140}Nd
^{108}Cd
^{220}U
^{80}Kr
^{248}Fm
Two equal touching spherical nuclei
^{272}108
^{300}120
Spherical nucleus

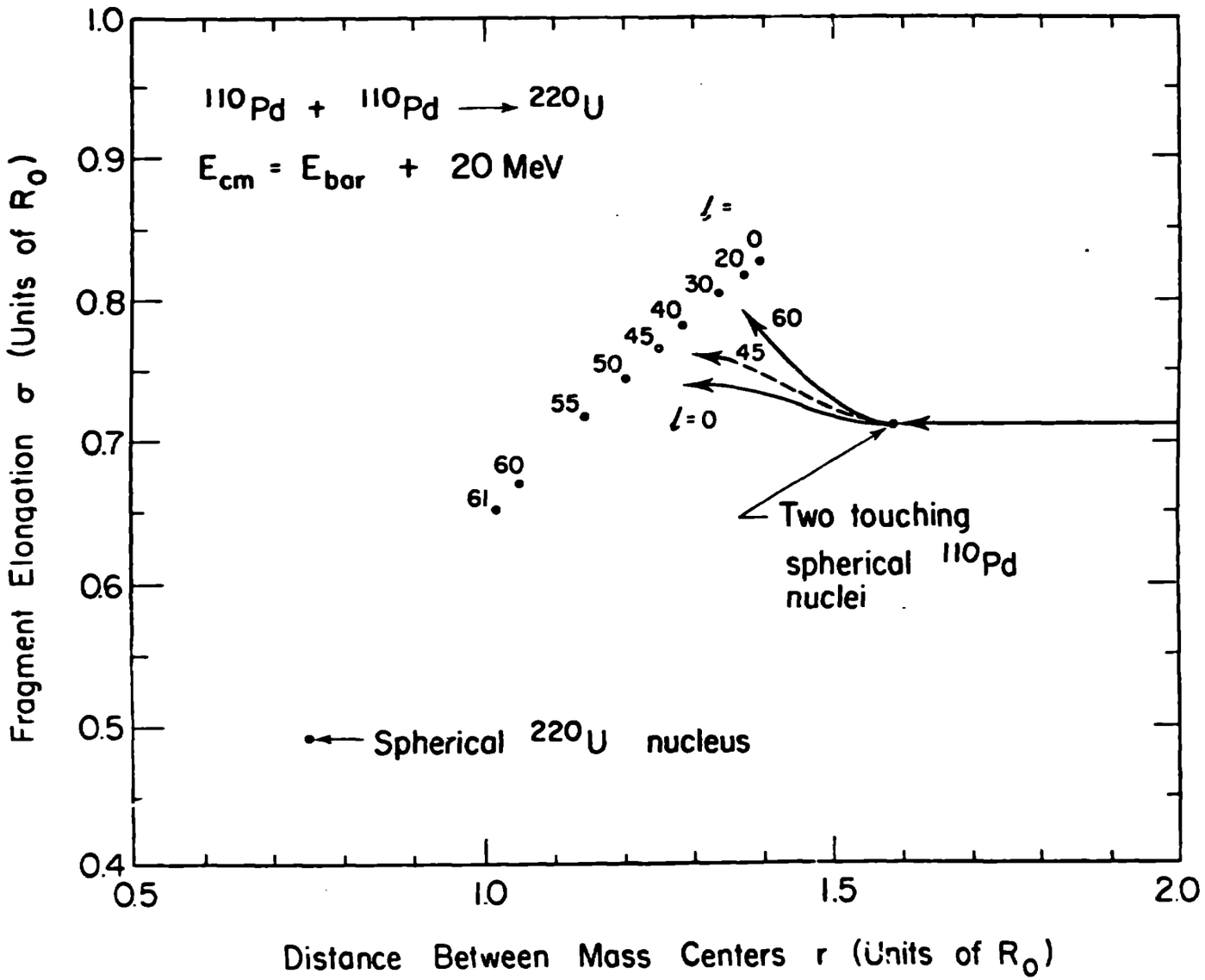
$^{110}Pd + {}^{110}Pd \longrightarrow {}^{220}U$
$E_{cm} = E_{bar} + 20$ MeV
l =
0
20
30
40
45
50
55
60
61
60
45
l = 0
Two touching spherical ^{110}Pd nuclei
Spherical ^{220}U nucleus
Fragment Elongation σ (Units of R_0)
Distance Between Mass Centers r (Units of R_0)
1.0
0.9
0.8
0.7
0.6
0.5
0.4
0.5
1.0
1.5
2.0

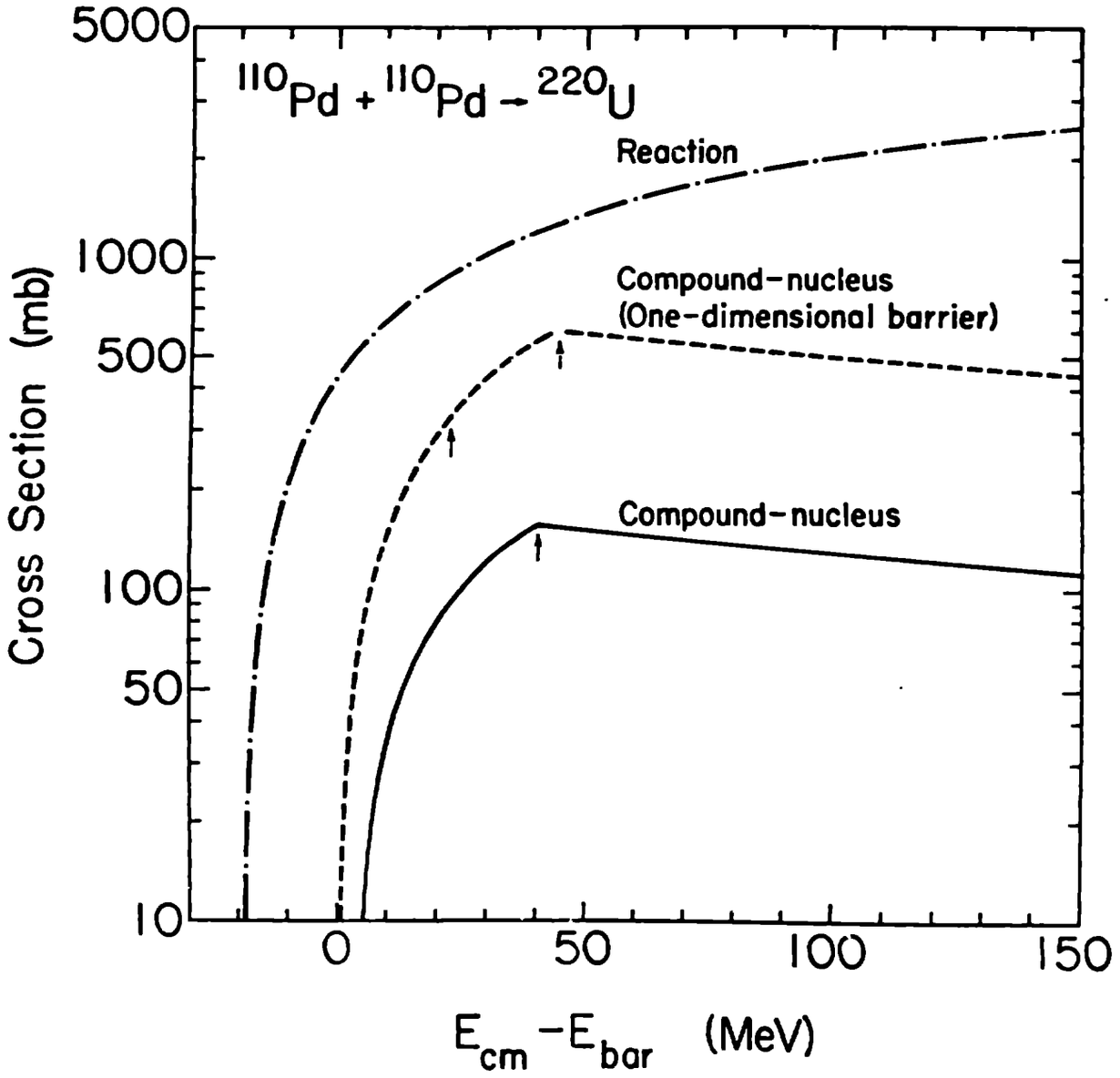
$^{110}Pd + ^{110}Pd \rightarrow ^{220}U$
Reaction
Compound-nucleus
(One-dimensional barrier)
Compound-nucleus
Cross Section (mb)
5000
1000
500
100
50
10
0
50
100
150
$E_{cm} - E_{bar}$ (MeV)

FIG. 1

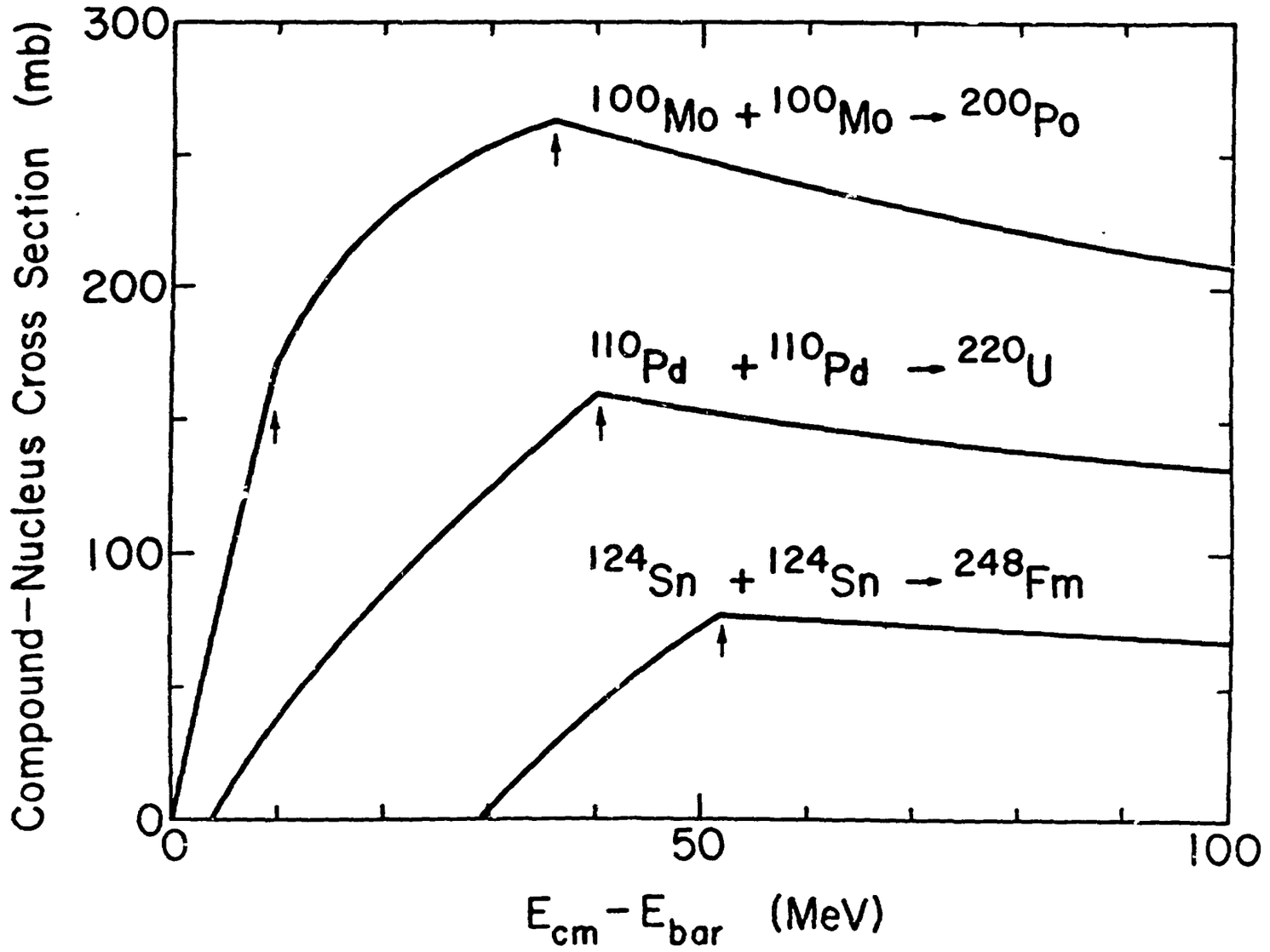
300
200
100
0
0
50
100
Compound-Nucleus Cross Section (mb)
$E_{cm} - E_{bar}$ (MeV)
$^{100}Mo + ^{100}Mo \rightarrow ^{200}Po$
$^{110}Pd + ^{110}Pd \rightarrow ^{220}U$
$^{124}Sn + ^{124}Sn \rightarrow ^{248}Fm$

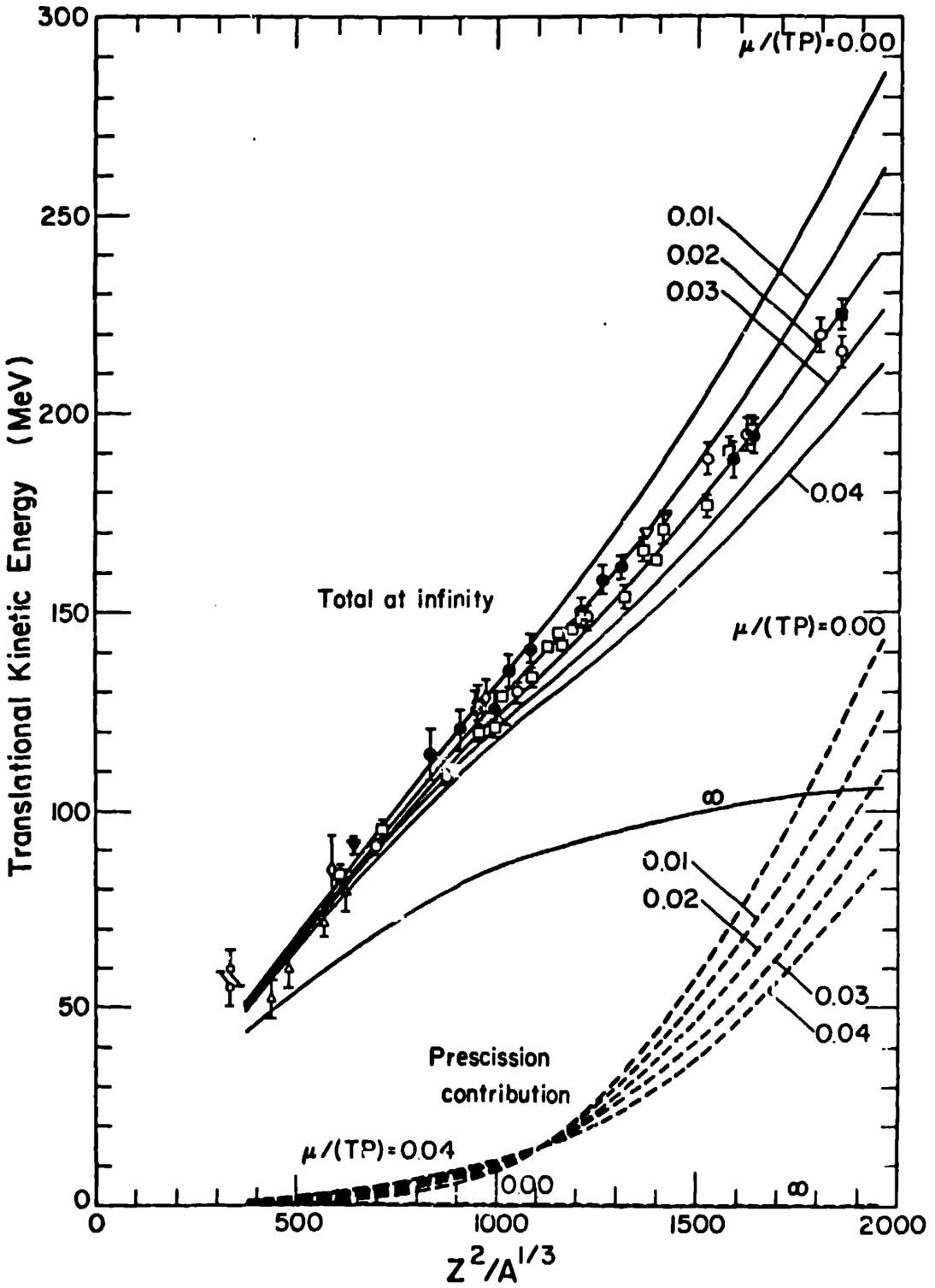
300
250
200
150
100
50
0
0
500
1000
1500
2000
Translational Kinetic Energy (MeV)
$Z^2/A^{1/3}$
μ/(TP)=0.00
0.01
0.02
0.03
0.04
Total at infinity
μ/(TP)=0.00
∞
0.01
0.02
0.03
0.04
Prescission
contribution
μ/(TP)=0.04
0.00
∞

Fig. 6

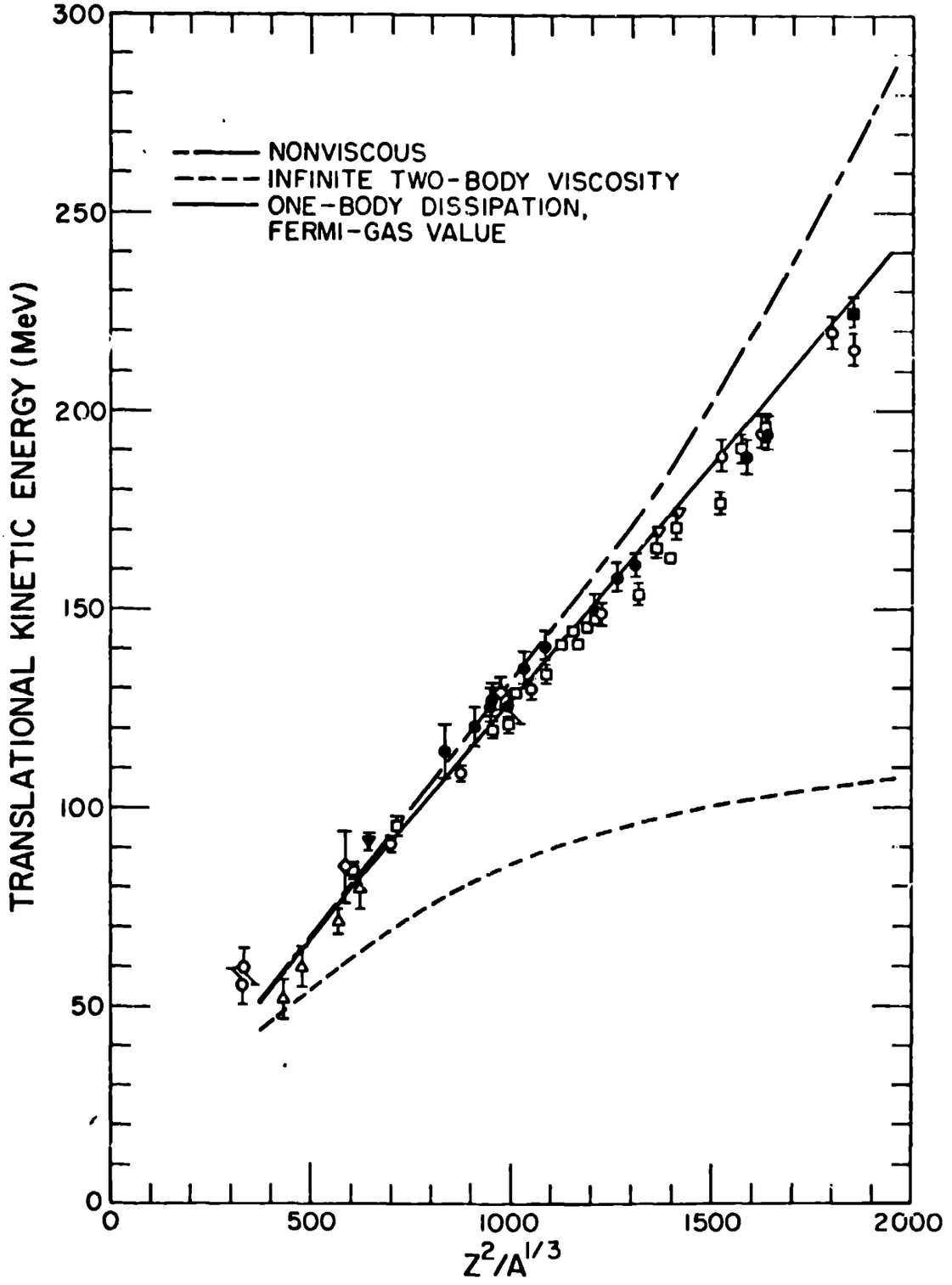
NONVISCOUS
INFINITE TWO-BODY VISCOSITY
ONE-BODY DISSIPATION,
FERMI-GAS VALUE
TRANSLATIONAL KINETIC ENERGY (MeV)
300
250
200
150
100
50
0
0
500
1000
1500
2000
$Z^2/A^{1/3}$

Fig. 7

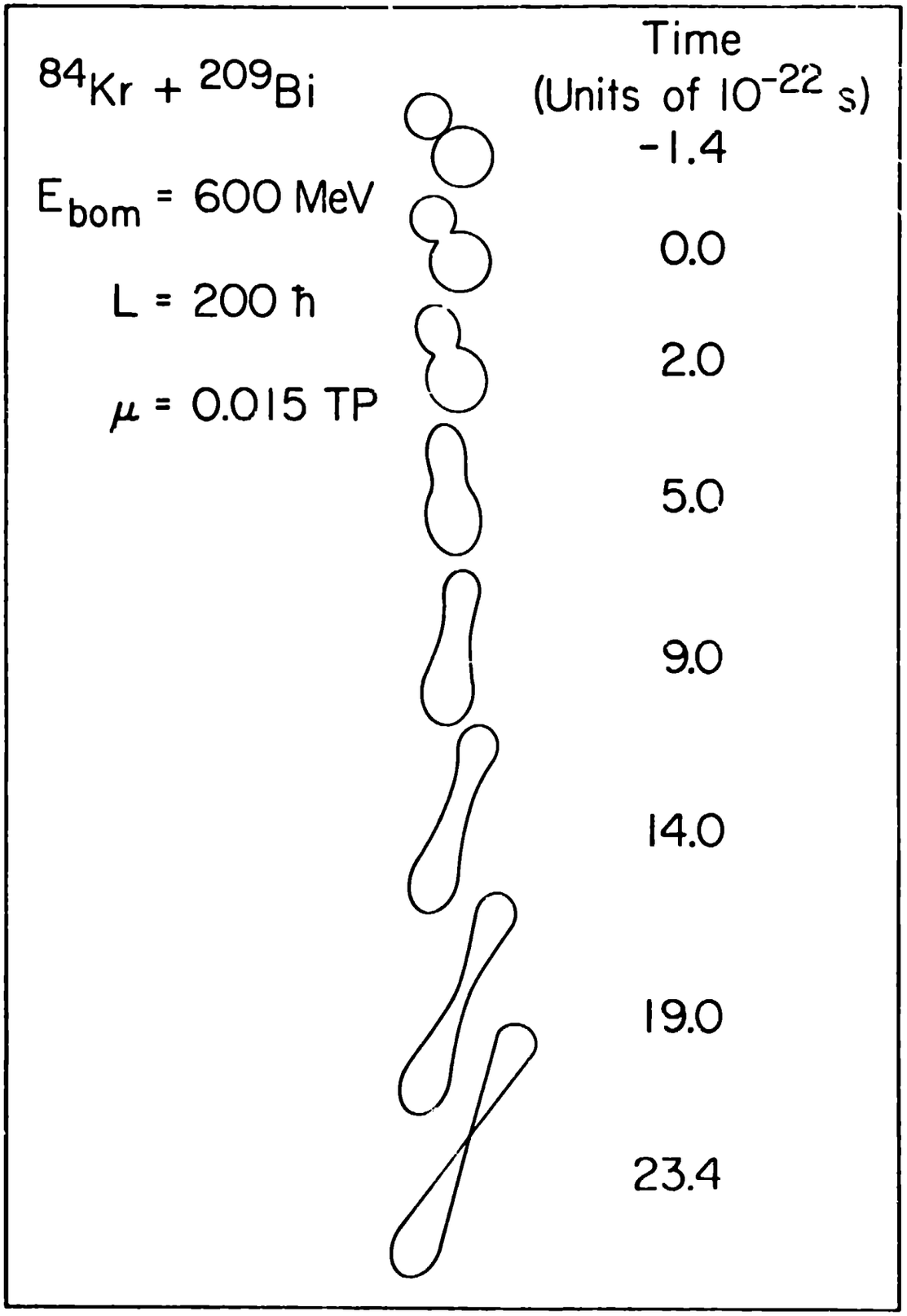
$^{84}Kr + ^{209}Bi$
E_{bom} = 600 MeV
L = 200 ħ
μ = 0.015 TP
Time
(Units of 10^{-22} s)
-1.4
0.0
2.0
5.0
9.0
14.0
19.0
23.4

Fig. 8